



Research article

Dexamethasone inhibits androgen receptor-negative prostate cancer cell proliferation via the GR-FOXO3a-GAS5 axis

Jieping Hu^{a,*}, Yanyan Hong^{b,1}, Xun Xie^a, Yuyang Yuan^a, Weipeng Liu^a, Bin Fu^{a,**}

^a Department of Urology, The First Affiliated Hospital, Jiangxi Medical College, Nanchang University, China

^b Department of Nursing, The First Affiliated Hospital, Jiangxi Medical College, Nanchang University, China

ARTICLE INFO

Keywords:

Androgen receptor
Glucocorticoid receptor
FOXO3a
LncRNA GAS5
Prostate cancer

ABSTRACT

Background: Studies have shown that glucocorticoid receptor (GR) has inconsistent effects on the proliferation of prostate cancer cells, we found dexamethasone inhibited the proliferation of androgen receptor-negative prostate cancer cells, but the underlying mechanisms remain to be illustrated.

Methods: GR expression and its prognosis role were analyzed based on the TCGA dataset. Bioinformatic analysis was performed to identify the candidate of GR downstream, which includes FOXO3a. After overexpressing FOXO3a in PC-3 cells, cell counting kit-8 (CCK-8) and migration assays were performed to evaluate cell proliferation and migration ability. Regulation of FOXO3a on GAS5 was also analyzed by JASPAR and PCR.

Results: GR had low expression in prostate cancer and predicted poor prognosis. FOXO3a was identified as the downstream of GR to inhibit the proliferation of prostate cancer cells. Moreover, FOXO3a directly induces GAS5 expression, forming the GR-FOXO3a-GAS5 signaling pathway.

Conclusion: Our study showed that GR played a role as a tumor suppressor gene in androgen receptor-negative prostate cancer cells via the GR-FOXO3a-GAS5 axis. Our results suggested patients with prostate cancer should be classified and develop a treatment plan according to the expression of AR and GR.

1. Introduction

Cancer incidence increased for prostate cancer by 3% annually, and it was estimated that 288,300 new cases, and 34,700 deaths in the US in 2023 [1]. Five-year relative survival could be almost 100% for localized and regional prostate cancer patients, but it would drop to 30% for patients with distant metastases [1]. Although advanced patients responded to initial anti-androgen therapy, most patients were no longer sensitive to treatment after 24–36 months and developed castration resistance prostate cancer (CRPC) [2]. Although many methods such as chemotherapy and immunotherapy are being studied, effective therapeutic measures are still lacking [3]. It is of great significance to study the mechanism of occurrence, development, and metastasis of prostate cancer, and the results would help identify specific prognostic molecular markers and new therapeutic targets.

* Corresponding author.

** Corresponding author.

E-mail addresses: hu_jieping@163.com (J. Hu), 792586870@qq.com (B. Fu).

¹ Contributed equally.

<https://doi.org/10.1016/j.heliyon.2024.e27568>

Received 11 January 2024; Received in revised form 29 February 2024; Accepted 1 March 2024

Available online 8 March 2024

2405-8440/© 2024 The Authors. Published by Elsevier Ltd. This is an open access article under the CC BY-NC-ND license (<http://creativecommons.org/licenses/by-nc-nd/4.0/>).

The etiology of prostate cancer is diverse, among which androgen receptor (AR) plays a crucial role in tumor growth. Since Huggins and Hodges discovered the androgen-dependent characteristics of prostate cancer in the 1940s, androgen deprivation therapy (ADT) has been applied clinically as an important therapeutic method for prostate cancer [4]. ADT includes two treatment methods: inhibition of testicular androgen secretion and inhibition of androgen activity. Inhibition of androgen secretion can be achieved through gonadotropin-releasing hormone agonists, antagonists, or surgical excision of the testis, etc., while the inhibition of androgen activity is to inhibit the binding of androgen to AR. In general, after the combination of androgen and AR, AR dimer is formed into the nucleus, which binds with androgen response elements to induce gene expression and promote the proliferation of tumor cells. However, the formation of CRPC indicates that even if androgen is at a very low castration level, AR can continue to activate downstream signaling pathways independent of androgen binding. AR amplification, mutation, spliceosome formation, and overexpression of AR coactivators can mediate the activation of AR signaling pathways [5]. In recent studies, it has been found that there are various factors for the progression of prostate cancer, and there is great heterogeneity in the formation mechanism of castration resistance in different patients [6]. Recently, it was reported that after continuous ADT treatment, prostate cancer cells gradually differentiate neuroendocrine, accompanied by decreased or even disappeared expression of AR, suggesting that AR-negative prostate cancer cells contribute to the progression of prostate cancer [2,6,7].

We previously studied the effect of glucocorticoid receptor (GR) on the proliferation of prostate cancer cells, GR did not affect cell proliferation in AR-positive cells but inhibited the proliferation of AR-negative cells [8]. LncRNA GAS5 participates in the regulation of dexamethasone on androgen receptor -negative and -positive prostate cancer cell proliferation, GR-induced GAS5 expression to inhibit the proliferation of AR-negative prostate cancer cells, and the combination of AR and GAS5 inhibited its effect in AR-positive cells [9], to further clarify the relationship between GR and GAS5, we used bioinformatics technology to analyze and screen the downstream of GR, we found that FOXO3a may act as a mediator between GR and GAS5, and experimentally verified that GR acted on GAS5 through FOXO3a to inhibit the proliferation of AR-negative prostate cancer cells.

2. Materials and methods

2.1. Bioinformatic and TCGA PRAD data analysis

Prostate cancer and glucocorticoid receptors were searched in the GEO (Genomic Expression Omnibus) database, and a total of 25 literatures were retrieved. We screened the articles one by one, and the inclusion criteria included: 1. GEO2R online analysis could be performed (16 articles); 2. GR agonists were used to treat prostate cancer cells (16-8 = 8 articles); The exclusion criteria included: 1. Less than 20 differentially expressed genes (GSE150437, GSE51872); 2. 2. Non-prostate cancer cells (GSE150432); 3. Only two groups of samples were compared (GSE71099); 4. Duplicate data (GSE39654 and GSE39880 for LNCaP-1F5 cell, GSE52169 and GSE51871 for LREX cell). Finally, two databases GSE39654 and GSE52169 were included for analysis. GTRD (Gene Transcription Regulation Database, <http://gtrd20-06.biouml.org/>) was used to predict GR downstream. For GTRD analysis, “Genes regulated by the specified transcription factor” was selected, the method was “analysis of TF binding”, TF binding site location was “promoter [-100, +10]”, organism was “Human”, transcription factor was “NR3C1 P04150”, the GR (NR3C1) downstream was then analyzed. TCGA PRAD Data included 497 prostate cancer patients, UALCAN (<https://ualcan.path.uab.edu/analysis.html>) was used to examine the expression of GR from the prostate adenocarcinoma (TCGA PRAD) database found in The Cancer Genome Atlas (TCGA) database. Survival analysis was done using UCSC Xena (<https://xenabrowser.net/heatmap/>) with TCGA Prostate Cancer (PRAD) dataset containing 550 samples. The human protein atlas (<https://www.proteinatlas.org/>) was used to analyze the GR and FOXO3 expression. The significance of expression levels between normal and tumors or tumor subtypes was calculated by *t*-test.

2.2. Cell lines

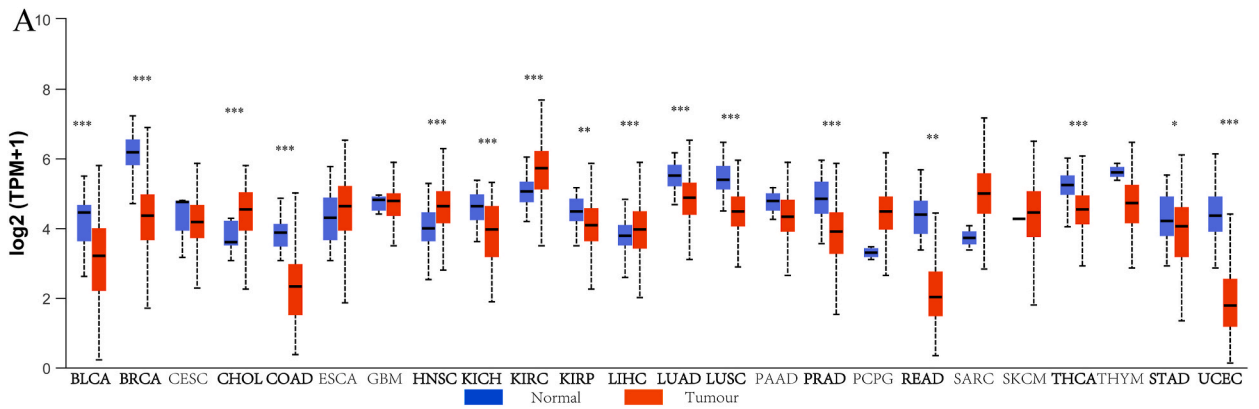
The human prostate cancer (PCa) cell lines PC-3 (American Type Culture Collection) were routinely maintained in RPMI 1640 (KGM31800S, keygentec, CA) with 10% fetal bovine serum (FBS, 10,099-141, keygentec, CA), 100 U/ml of penicillin, and 100 mg/mL of streptomycin in a 5% CO₂ atmosphere at 37 °C. Dexamethasone was dissolved in DMSO with 2×10^{-2} M concentration, dexamethasone should be diluted 100,000-fold in medium to reach a final concentration of 100 nM. PC-3 cells infected with FOXO3a overexpressing lentiviral vector were prepared for plate infection when the cells grew to the appropriate density. The 6-well plate was taken as an example, and 1×10^5 cells were laid in each hole. Cell infection was carried out after cell adhesion on the second day. The polycoagulant was added into the medium at the rate of 2000, and the amount of virus required for each group was calculated according to the formula of “amount of virus added per well (μl) = MOI × cell number/titer (TU/ml) × 1000”, which was added into the culture medium, mixed and added into the well for cell infection, and PCR and WB were performed 72h later to verify the infection efficiency.

2.3. Real time-PCR

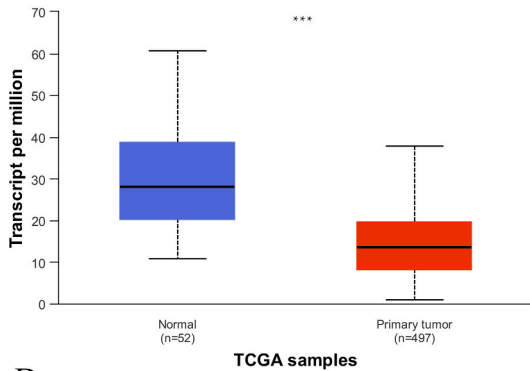
Fluorescence quantitative PCR verification RNA was extracted from each group. After extracting RNA, cDNA was synthesized according to the corresponding reverse transcription kit (CW0581 M, CWBIO). cDNA was used as the template for detection on the real-time quantitative PCR instrument. Primers are as follows:

β-actin F TGGCACCCAGCACAATGAA

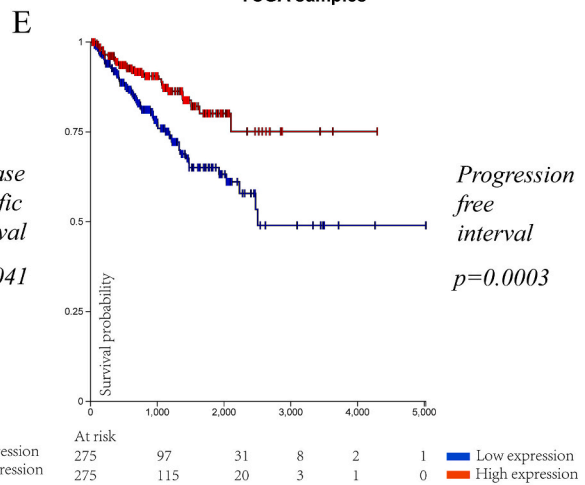
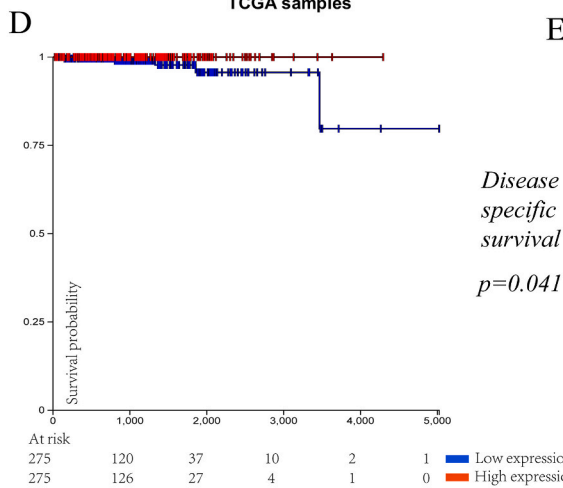
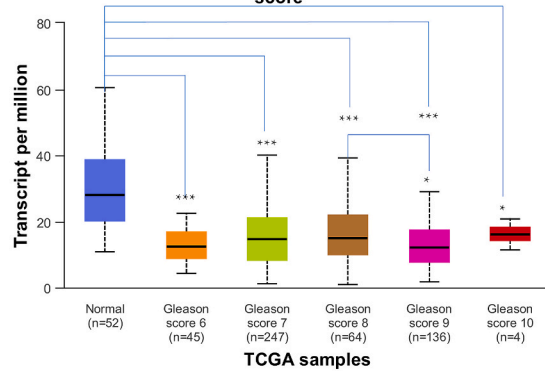
β-actin R CTAAGTCATAGTCCGCCTAGAAGCA.



B Expression of NR3C1 in PRAD based on Sample types



C Expression of NR3C1 in PRAD based on patient's gleason score



(caption on next page)

Fig. 1. NR3C1 gene expression and prognosis study using TCGA dataset. (A) Boxplots show the expression of the NR3C1 gene in tumors (red) and normal (blue) in 24 tumors (Bladder urothelial carcinoma [BLCA] Normal (n = 19) VS Tumor (n = 408); Breast invasive carcinoma [BRCA] Normal (n = 114) VS Tumor (n = 1097); Cervical squamous cell carcinoma [CESC] Normal (n = 3) VS Tumor (n = 305); Cholangiocarcinoma [CHOL] Normal (n = 9) VS Tumor (n = 36); Colon adenocarcinoma [COAD] Normal (n = 41) VS Tumor (n = 286); Esophageal carcinoma [ESCA] Normal (n = 11) VS Tumor (n = 184); Glioblastoma multiforme [GBM] Normal (n = 5) VS Tumor (n = 156); Head and neck squamous cell carcinoma [HNSC] Normal (n = 44) VS Tumor (n = 520); Kidney chromophobe [KICH] Normal (n = 25) VS Tumor (n = 67); Kidney renal clear cell carcinoma [KIRC] Normal (n = 72) VS Tumor (n = 533); Kidney renal papillary cell carcinoma [KIRP] Normal (n = 32) VS Tumor (n = 290); Liver hepatocellular carcinoma [LIHC] Normal (n = 50) VS Tumor (n = 371); Lung adenocarcinoma [LUAD] Normal (n = 59) VS Tumor (n = 515); Lung squamous cell carcinoma [LUSC] Normal (n = 52) VS Tumor (n = 503); Pancreatic adenocarcinoma [PAAD] Normal (n = 4) VS Tumor (n = 178); Prostate adenocarcinoma [PRAD] Normal (n = 52) VS Tumor (n = 497); Pheochromocytoma and paraganglioma [PCPG] Normal (n = 3) VS Tumor (n = 179); Rectal adenocarcinoma [READ] Normal (n = 10) VS Tumor (n = 166); Sarcoma [SARC] Normal (n = 2) VS Tumor (n = 260); Skin cutaneous melanoma [SKCM] Normal (n = 1) VS Tumor (n = 472); Thyroid carcinoma [THCA] Normal (n = 59) VS Tumor (n = 505); Thymoma [THYM] Normal (n = 2) VS Tumor (n = 120); Stomach adenocarcinoma [STAD] Normal (n = 34) VS Tumor (n = 415); Uterine corpus endometrial carcinoma [UCEC] Normal (n = 35) VS Tumor (n = 546)). (B) Boxplot showing the expression of the NR3C1 gene by RNA-seq in normal tissue (blue) and Pca tumor (red) tissue. (C) Correlation of the expression of NR3C1 RNA with patient Gleason scores. (D) Disease-specific survival analysis of 550 Pca patients according to GR expression. (E) Progression-free interval was compared between GR high and low expression. (Asterisks denote significant p-values; *p < 0.05, **p < 0.01 and *** indicates p < 0.001).

FOXO3A F CGGACAAACGGCTCACTCT.

FOXO3A R GGACCCGCATGAATCGACTAT.

LncRNAGAS5 F CTTGGGTAAGGACATGAAGACA.

LncRNAGAS5 R AAGACCACTGGGAGGCTGAG.

Note: Primer synthesis company: General Biological Systems (Anhui) Co., LTD.

2.4. Western blot

Each group of cells was added into lysate, and the homogenate was collected by 12000r/min high-speed centrifuge for 15min. The supernatant was taken to obtain the protein. Protein concentration was determined according to the BCA kit (E-BC-K318-M, Elabscience), after protein denaturation, sodium dodecyl sulfate gel electrophoresis was performed for 1–2 h, and the proteins were transferred by wet method for 120 min. Incubation with primary antibody solution at 4 °C overnight; The secondary antibody solution was incubated at room temperature for 1 h. The ECL exposure solution is dripped onto the membrane and exposed in an imaging system. The information of antibody was: Mouse Monoclonal Anti-β-Actin (TA-09, ZS-BIO, 1/2000), Secondary antibody: Goat Anti-Mouse IgG (H + L) (ZB-2305, ZS-BIO, 1/2000), Rabbit Anti FOXO3A (AF7624, Affinity, 1/1000); Second antibody: Goat Anti-Rabbit IgG (H + L) (ZB-2301, ZS-BIO, 1/2000).

2.5. CCK8 assay

By CCK8 detection, cells were digested, suspended, counted, and planed, and the cell density was 1×10^4 cells per well; After 24 h, the CCK8 test was performed, and the 96-well plate cells to be tested were replaced with the same medium, 100ul per hole. Add 10ul CCK8 reagent (KGA317, keygentec, CA) to each well and incubate in the incubator for 2 h. The light absorption value was detected by the enzyme-labeler at 450 nm wavelength.

$$\text{Cell viability (\%)} = \frac{A (\text{experimental group}) - A (\text{blank medium})}{A (\text{control group}) - A (\text{blank medium})} \times 100\%.$$

2.6. Migration assay

Cells (5×10^4 for PC3) after different treatments were re-suspended with serum-free media and seeded in the upper chambers of the transwells. 10% FBS with or without 100 nM Dexamethasone was put in the lower chambers. After 24 h of incubation, remove the medium in the hole, then add PBS to clean for 5 min, and add 0.1% crystal violet to the prepared chamber and stand for dyeing for 1 h. After dyeing, wipe the inner cells of the chamber with a cotton swab, and place the chamber upside down on a slide to take photos. After taking photos, remove the staining solution in the hole. The dye solution of 33% acetic acid 1 mL in lysed cells was added to each well, thoroughly mixed, and left to stand, and 200 μl was absorbed from each well and placed in a 96-well plate. The wavelength was 562 nm with a multifunctional enzyme marker. The light absorption value of the solution in each well was determined using 200 μl 33% acetic acid per well as a control.

2.7. Statistical analysis

All experiments were repeated three times, the quantitative results were expressed as mean ± standard deviation. T-test was used for comparison between the two groups, F test was performed to compare variances, and $p < 0.05$ was regarded as significant. SPSS 26.0 and GraphPad Prism 8 software were used for statistical analysis.

3. Results

3.1. GR is low expression in prostate cancer and associated with prognosis

The TCGA database showed that GR expression was down-regulated in a variety of tumors compared with normal tissues. Such as Bladder Urothelial Carcinoma (BLCA), Breast invasive carcinoma (BRCA), Colon adenocarcinoma (COAD), Uterine Corpus Endometrial Carcinoma (UCEC) and so on (Fig. 1A). In prostate adenocarcinoma (PRAD), the expression of GR was significantly lower in tumor tissue as compared to normal (median 13.639 VS 28.015, $p < 0.001$, Fig. 1B). The GR expression of each Gleason score group was also lower than normal tissue (Fig. 1C). Survival analysis showed that prostate cancer patients with high GR expression had longer disease-specific survival and progression-free intervals than those with low GR expression (Fig. 1D and E). These results are consistent with our previous studies that dexamethasone inhibits the proliferation of prostate cancer cells [8].

3.2. Bioinformatic analysis indicates FOXO3a as GR downstream in prostate cancer

Bioinformatics technology was used to analyze and screen GR downstream, and prostate cancer and glucocorticoid receptors were searched in the GEO database. A total of 25 literatures were retrieved, and two databases were included in the analysis and screening. The GSE39654 data were obtained by microarray expression assays (GSE39654: Expression profiling by microarray of LNCaP-1F5 cells treated with vehicle, 100 nM 5 α -dihydrotestosterone (DHT), 100 nM dexamethasone (Dex), 1000 nM cyproterone acetate (CPA), 100 nM mifepristone (RU486) and combination of 100 nM DHT, 100 nM Dex for 24 h). LNCaP-1F5 cells were obtained from LNCaP cells transfected with rabbit GR. The stable expression of AR and GR was identified, and the expression of AR downstream genes was not affected. The GSE52169 database was derived from the LREX cell line treated with dexamethasone under the condition of enzalutamide (castration-resistant cell line treated with MDV3100 in LNCaP cells). 32 overlapping differentially expressed mRNAs were obtained by analysis and screening of the two sets of data, and the downstream GR was predicted by combining GTRD (biouml.org), further analysis showed that 23 possible downstream genes of GR may be related to the function of GR. (Fig. 2A). The heat map showed that the expression of those 23 overlapping genes in the GSE52169 changed upon dexamethasone treatment. Dexamethasone increased the expression level of FOXO3a by about 2 times (Fig. 2B and D). GSE39654 showed an approximately three-fold increase in FOXO3a expression in LNCaP-1F5 cells treated with dexamethasone (Fig. 2C).

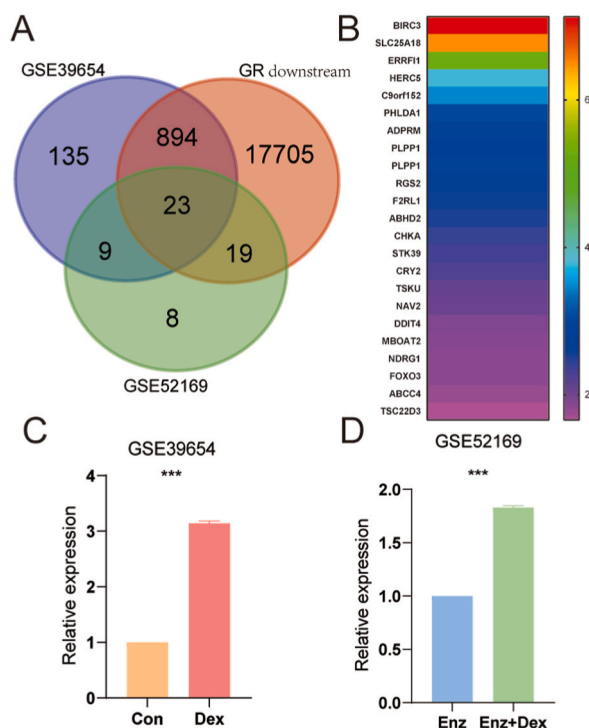


Fig. 2. Bioinformatic analysis GR downstream in prostate cancer. (A) Two databases (GSE39654 and GSE52169) were included in the analysis and screening. 32 overlapping differentially expressed mRNAs were obtained by analysis and screening of the two sets of data, and the GR downstream was predicted by combining GTRD (biouml.org), 23 possible downstream genes of GR were involved in the formation of castration resistance. (B) The heat map showed that the expression changes of 23 overlapping molecules of dexamethasone in the GSE52169 database. (C) GSE39654 showed an approximately three-fold increase in FOXO3a expression in LNCaP-1F5 cells treated with dexamethasone. (D) Dexamethasone increased the expression level of FOXO3a by about 2 times in GSE52169. (Asterisks denote significant p-values; *** indicates $p < 0.001$).

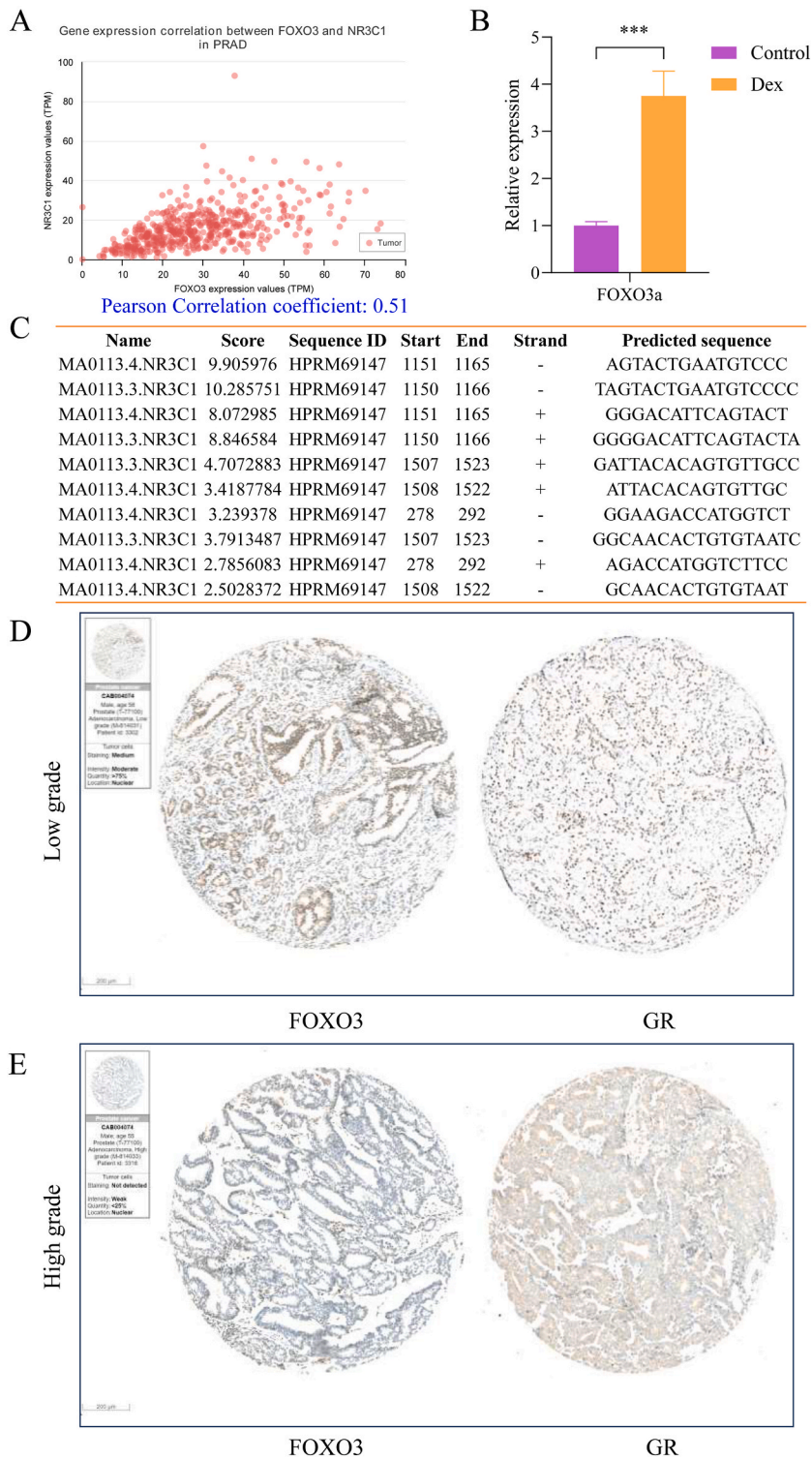


Fig. 3. Clinicopathology analysis between GR and FOXO3a. (A) Gene expression correlation between FOXO3a and GR in PCa. (B) FOXO3a mRNA was detected after dexamethasone treatment. (C) JASPAR website predicted promoter binding sites of GR and FOXO3a. (D) A represent 56-year-old low-grade PCa patient had a consistent high expression of GR and FOXO3a. (E) A represent 55-year-old high-grade PCa patient had a consistent low expression of GR and FOXO3a. (Asterisks denote significant p-values; *** indicates $p < 0.001$).

3.3. Clinicopathological findings suggest that GR is associated with FOXO3a expression

Person correlation analysis found that GR expression was significantly correlated with FOXO3a (Fig. 3A), and dexamethasone treatment of prostate cancer PC-3 cells also showed elevated FOXO3a expression (Fig. 3B). FOXO3a has multiple promoter sequences (listed on the igenebio website: HPRM69145, HPRM69146, HPRM69147, HPRM69148, HPRM69149, HPRM43701), we used the JASPAR database to analyze the relationship between GR and FOXO3a. GR was found to bind to the promoter sequence region HPRM69147 (Fig. 3C). We selected two typical cases from the human protein atlas website and analyzed GR and FOXO3a expression. Fig. 3D showed a 58 years old male with low-grade prostate adenocarcinoma, the expression of GR and FOXO3a was consistent and high, what's more, the expression of GR and FOXO3a was consistent and lower in a 55 years old patient who suffered from high-grade prostate adenocarcinoma (Fig. 3E).

3.4. FOXO3a inhibits prostate cancer cell proliferation

To clarify the effect of FOXO3a on prostate cancer cells, we overexpressed FOXO3a in PC-3 cells, and PCR showed a significant increase in mRNA expression (Fig. 4A), WB showed successful overexpression of FOXO3a protein (Fig. 4B), CCK8 detection showed decreased cell viability (Fig. 4C), and migration experiment showed decreased cell migration ability (Fig. 4D and E).

3.5. GAS5 is induced by FOXO3a and responsible for the GR-FOXO3a-GAS5 axis

To further determine the relationship between FOXO3a and GAS5, we used JASPAR to predict the promoter binding sites of FOXO3a and GAS5 online and found that there were 10 binding regions between FOXO3a and GAS5, and most of the scores were greater than 5 (Fig. 5A), indicating that FOXO3a may directly regulate the expression of GAS5. The expression of GAS5 was increased in PC-3 cells overexpressing FOXO3a (Fig. 5B), and the expression level of GAS5 was also significantly increased in PC-3 cells treated with dexamethasone (Fig. 5C). Therefore, we believe that GR promotes the expression of FOXO3a, and then directly induces the expression of GAS5, which inhibits the proliferation of AR-negative cells (Fig. 5D).

4. Discussion

Glucocorticoids play a role through GR. Structurally, GR is similar to AR, divided into N-terminal domain, DNA domain, and ligand domain. After glucocorticoids bind to the ligand domain of GR in the cytoplasm, GR forms a dimer and enters the nucleus. By binding to the Glucocorticoid receptor element (GRE), it regulates gene expression, thereby regulating cell proliferation [10]. In terms of

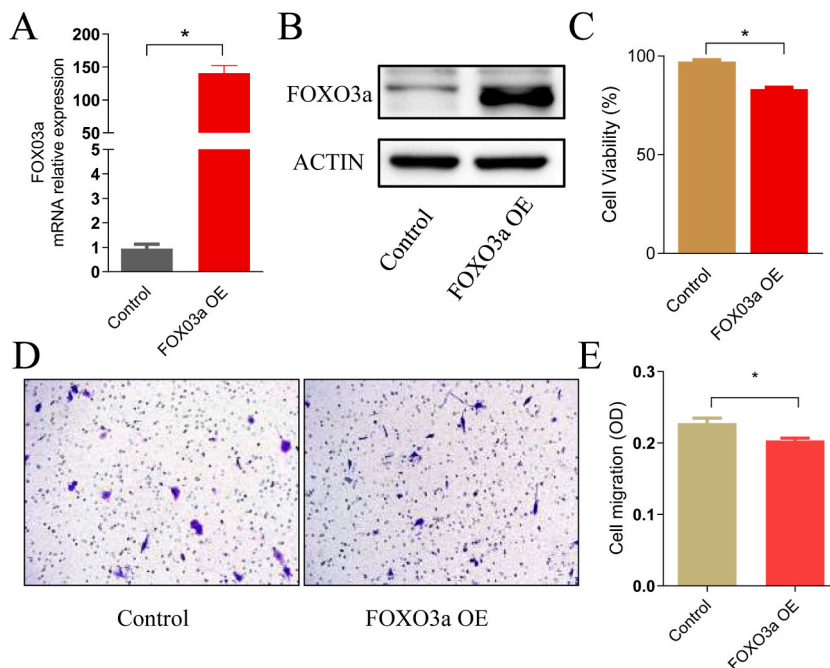


Fig. 4. FOXO3a inhibits prostate cancer cell proliferation and migration. (A) FOXO3a was overexpressed in PC-3 cells, and PCR showed a significant increase in mRNA expression. (B) Western blot showed successful overexpression of FOXO3a protein. (C) CCK8 assay showed decreased cell viability after FOXO3a overexpression. (D) Cell migration assay showed decreased cell migration ability after FOXO3a overexpression. (E) The OD value was compared between the control and FOXO3a overexpression groups. (Asterisks denote significant p-values; * $p < 0.05$).

cancer tissues is relatively low initially, while the effect of AR is inhibited during ADT treatment, and the expression of GR graduated increased. The combination of GR and GRE activates AR downstream genes through the bypass pathway and promotes the progression of prostate cancer [14,16]. These results indicate that there is an extremely complex relationship between GR and AR, and the interaction between them affects the occurrence and development of prostate cancer. In this study, we found GR high expression was associated with better prognosis, and we first prompted that GR inhibited the proliferation of AR-negative prostate cancer cells via the GR-FOXO3a-GAS5 axis. Patients with prostate cancer should be classified and develop a treatment plan according to the expression of AR and GR.

The effects of FOXO3a were also varied. Cell experiments conducted in Du145 cells found that inhibition of the Akt signal can promote the entry of FOXO3a into the nucleus and induce cell apoptosis [17]. The study on TRAMP, a transgenic mouse model of prostate cancer, found that tumor progression was accompanied by the activation of the Akt and the inhibition of FOXO3a activity. Feeding TRAMP rats with FOXO3a inhibitors can promote the progression of tumors, indicating that FOXO3a may inhibit the cell growth of prostate cancer [18]. Studies have shown that the expression level of cytoplasm FOXO3a was directly proportional to the Gleason score of prostate cancer [19]. In LNCaP cells, FOXO3a may also promote cell proliferation through AR [20,21]. However, our study found that FOXO3a inhibited the proliferation and migration of AR-negative prostate cancer cells. These data suggested that FOXO3a may play a dual role in the proliferation of prostate cancer, and this role may be related to the level of AR expression in cells. It was noted that the reduction in cell migration may be confounded by cytotoxicity as the FOXO3a overexpression results in significantly lower cell viability, the detection of some epithelial-mesenchymal transition markers can help to demonstrate changes in cell migration ability.

The regulatory mechanism of GR on FOXO3a remains to be further demonstrated. Our results suggested GR may play a regulatory role by binding the promoter of FOXO3a. The combination of GR and FOXO3a promoter region or FOXO3a protein interaction was found in the JASPAR transcription prediction website. Our laboratory will conduct experiments to further verify the relationship between GR and FOXO3a, the regulatory mechanism of FOXO3a on GAS5 will also be verified by experiments such as luciferase gene reporting experiments. In addition, the invasion and metastasis ability and mechanism of GR for AR-negative prostate cancer cells are also worthy of further study.

5. Conclusion

Our study showed that GR played a role as a tumor suppressor gene in AR-negative prostate cancer cells, and GR induced FOXO3a expression and acted in a proliferative inhibitory role by directly inducing GAS5.

Funding/Support and role of the sponsor

This study was supported by Jiangxi Provincial Natural Science Foundation (No: 20202BAB216033).

Data availability statement

The datasets used and analyzed during the current study available from the corresponding author on reasonable request.

Ethics approval

The research complies with the guidelines for human studies and was conducted ethically in accordance with the World Medical Association Declaration of Helsinki.

CRedit authorship contribution statement

Jieping Hu: Writing – original draft, Software, Methodology, Investigation, Funding acquisition, Data curation, Conceptualization. **Yanyan Hong:** Methodology, Investigation, Data curation. **Xun Xie:** Methodology, Data curation. **Yuyang Yuan:** Investigation, Data curation. **Weipeng Liu:** Investigation, Formal analysis. **Bin Fu:** Writing – review & editing, Supervision, Project administration, Conceptualization.

Declaration of competing interest

The authors declare that they have no known competing financial interests or personal relationships that could have appeared to influence the work reported in this paper.

Appendix A. Supplementary data

Supplementary data to this article can be found online at <https://doi.org/10.1016/j.heliyon.2024.e27568>.

References

- [1] R.L. Siegel, K.D. Miller, N.S. Wagle, A. Jemal, Cancer statistics, 2023, *CA A Cancer J. Clin.* 73 (1) (2023) 17–48, <https://doi.org/10.3322/caac.21763>.
- [2] A. Jamroze, G. Chatta, D.G. Tang, Androgen receptor (AR) heterogeneity in prostate cancer and therapy resistance, *Cancer Lett.* 518 (2021) 1–9, <https://doi.org/10.1016/j.canlet.2021.06.006>.
- [3] M. Cai, X.L. Song, X.A. Li, M. Chen, J. Guo, D.H. Yang, et al., Current therapy and drug resistance in metastatic castration-resistant prostate cancer, *Drug Resist. Updates : reviews and commentaries in antimicrobial and anticancer chemotherapy* 68 (2023) 100962, <https://doi.org/10.1016/j.drug.2023.100962>.
- [4] C. Huggins, C.V. Hodges, *Studies on prostatic cancer. I. The effect of castration, of estrogen and of androgen injection on serum phosphatases in metastatic carcinoma of the prostate*, 1941, *J. Urol.* 167 (2 Pt 2) (2002) 948–951. ; discussion 52.
- [5] D. Senapati, V. Sharma, S.K. Rath, U. Rai, N. Panigrahi, Functional implications and therapeutic targeting of androgen response elements in prostate cancer, *Biochimie* (2023), <https://doi.org/10.1016/j.biochi.2023.07.012>.
- [6] D.G. Tang, Understanding and targeting prostate cancer cell heterogeneity and plasticity, *Semin. Cancer Biol.* 82 (2022) 68–93, <https://doi.org/10.1016/j.semcancer.2021.11.001>.
- [7] X. Shui, R. Xu, C. Zhang, H. Meng, J. Zhao, C. Shi, Advances in neuroendocrine prostate cancer research: from model construction to molecular network analyses, *Laboratory investigation; a journal of technical methods and pathology* 102 (4) (2022) 332–340, <https://doi.org/10.1038/s41374-021-00716-0>.
- [8] J. Guo, K. Ma, H.M. Xia, Q.K. Chen, L. Li, J. Deng, et al., Androgen receptor reverts dexamethasone-induced inhibition of prostate cancer cell proliferation and migration, *Mol. Med. Rep.* 17 (4) (2018) 5887–5893, <https://doi.org/10.3892/mmr.2018.8566>.
- [9] J. Hu, J. Deng, R. Cao, S. Xiong, J. Guo, LncRNA GAS5 participates in the regulation of dexamethasone on androgen receptor -negative and -positive prostate cancer cell proliferation, *Mol. Cell. Probes* 53 (2020) 101607, <https://doi.org/10.1016/j.mcp.2020.101607>.
- [10] J. Hu, Q. Chen, The role of glucocorticoid receptor in prostate cancer progression: from bench to bedside, *Int. Urol. Nephrol.* 49 (3) (2017) 369–380, <https://doi.org/10.1007/s11225-016-1476-8>.
- [11] H. Butz, A. Patócs, Mechanisms behind context-dependent role of glucocorticoids in breast cancer progression, *Cancer Metastasis Rev.* 41 (4) (2022) 803–832, <https://doi.org/10.1007/s10555-022-10047-1>.
- [12] A. Yemelyanov, J. Czworonog, D. Chebotaev, A. Karseladze, E. Kulevitch, X. Yang, et al., Tumor suppressor activity of glucocorticoid receptor in the prostate, *Oncogene* 26 (13) (2007) 1885–1896, <https://doi.org/10.1038/sj.onc.1209991>.
- [13] K. Cheng, X. Liu, L. Chen, J.M. Lv, F.J. Qu, X.W. Pan, et al., α -Viniferin activates autophagic apoptosis and cell death by reducing glucocorticoid receptor expression in castration-resistant prostate cancer cells, *Med. Oncol.* 35 (7) (2018) 105, <https://doi.org/10.1007/s12032-018-1163-y>.
- [14] V.K. Arora, E. Schenkein, R. Murali, S.K. Subudhi, J. Wongvipat, M.D. Balbas, et al., Glucocorticoid receptor confers resistance to antiandrogens by bypassing androgen receptor blockade, *Cell* 155 (6) (2013) 1309–1322, <https://doi.org/10.1016/j.cell.2013.11.012>.
- [15] M. Sakellakis, L.J. Flores, Is the glucocorticoid receptor a key player in prostate cancer?: a literature review, *Medicine* 101 (29) (2022) e29716, <https://doi.org/10.1097/md.00000000000029716>.
- [16] F. Zhou, Y. Shi, G. Zhao, S. Aufderklamm, K.S. Murray, B. Jin, A narrative review of the role of glucocorticoid receptors in prostate cancer: developments in last 5 years, *Transl. Androl. Urol.* 11 (8) (2022) 1189–1199, <https://doi.org/10.21037/tau-22-501>.
- [17] D. Waseem, G.M. Khan, I.U. Haq, U. Rashid, D.N. Syed, The triphenyltin carboxylate derivative triphenylstannyl 2-(benzylcarbamoyl)benzoate impedes prostate cancer progression via modulation of Akt/FOXO3a signaling, *Toxicol. Appl. Pharmacol.* 401 (2020) 115091, <https://doi.org/10.1016/j.taap.2020.115091>.
- [18] S. Shukla, N. Bhaskaran, G.T. Maclennan, S. Gupta, Deregulation of FoxO3a accelerates prostate cancer progression in TRAMP mice, *Prostate* 73 (14) (2013) 1507–1517, <https://doi.org/10.1002/pros.22698>.
- [19] S. Shukla, M. Shukla, G.T. Maclennan, P. Fu, S. Gupta, Deregulation of FOXO3A during prostate cancer progression, *Int. J. Oncol.* 34 (6) (2009) 1613–1620, <https://doi.org/10.3892/ijo.00000291>.
- [20] S. Wang, N. Wang, B. Yu, M. Cao, Y. Wang, Y. Guo, et al., Circulating IGF-1 promotes prostate adenocarcinoma via FOXO3A/BIM signaling in a double-transgenic mouse model, *Oncogene* 38 (36) (2019) 6338–6353, <https://doi.org/10.1038/s41388-019-0880-9>.
- [21] L. Yang, S. Xie, M.S. Jamaluddin, S. Altuwaijri, J. Ni, E. Kim, et al., Induction of androgen receptor expression by phosphatidylinositol 3-kinase/Akt downstream substrate, FOXO3a, and their roles in apoptosis of LNCaP prostate cancer cells, *J. Biol. Chem.* 280 (39) (2005) 33558–33565, <https://doi.org/10.1074/jbc.M504461200>.